Thermally induced charge current through long molecules

Natalya A. Zimbovskaya, and Abraham Nitzan

Citation: The Journal of Chemical Physics **148**, 024303 (2018);
View online: https://doi.org/10.1063/1.5005057
View Table of Contents: http://aip.scitation.org/toc/jcp/148/2
Published by the American Institute of Physics

Thermally induced charge current through long molecules

Natalya A. Zimbovskaya[1] and Abraham Nitzan[2,3]
[1]*Department of Physics and Electronics, University of Puerto Rico, Humacao, Puerto Rico 00791, USA*
[2]*Department of Chemistry, University of Pennsylvania, Philadelphia, Pennsylvania 19104, USA*
[3]*School of Chemistry, Tel Aviv University, Tel Aviv, Israel*

(Received 16 September 2017; accepted 22 December 2017; published online 10 January 2018)

In this work, we theoretically study steady state thermoelectric transport through a single-molecule junction with a long chain-like bridge. Electron transmission through the system is computed using a tight-binding model for the bridge. We analyze dependences of thermocurrent on the bridge length in unbiased and biased systems operating within and beyond the linear response regime. It is shown that the length-dependent thermocurrent is controlled by the lineshape of electron transmission in the interval corresponding to the HOMO/LUMO transport channel. Also, it is demonstrated that electron interactions with molecular vibrations may significantly affect the length-dependent thermocurrent. *Published by AIP Publishing.* https://doi.org/10.1063/1.5005057

I. INTRODUCTION

Presently, charge transport through molecular systems is an important research field because of possible applications of these systems in molecular electronics.[1–4] The key element and basic building block of molecular electronic devices is a single-molecule junction including a couple of metallic/semiconducting electrodes linked by a molecular bridge. Alongside other tailored nanoscale systems (such as carbon-based nanostructures and quantum dots), single-molecule junctions hold promise for enhanced efficiency of heat-to-electric energy conversion.[5–12] Therefore, thermoelectric properties of single-molecule junctions are being explored both theoretically and experimentally.

In general, thermoelectric charge transport through molecular junctions is controlled by simultaneous driving by electric and thermal driving forces. The combined effect of these forces depends on several factors including the bridge geometry and the characteristics of its coupling to the leads[13–24] and electron-electron interactions.[25–34] Thermoelectric transport characteristics may be affected due to the interaction between transmitting electrons and environmental nuclear motions[35–54] and the effects of quantum interference.[55,56] Electron-photon interactions may also bring changes in thermoelectric properties of nanoscale systems.[57] Under certain conditions (e.g., in single-molecule junctions with ferromagnetic electrodes and/or with a magnetic molecule used as a linker), spin polarization of electrons may significantly influence thermoelectric transport resulting in several new phenomena such as the spin Seebeck effect.[58–69]

It was repeatedly demonstrated that electron transport through molecules strongly depends on the molecular length. Length-dependent electronic conductance as well as the electronic contribution to heat conductance and thermoelectric response were observed and discussed in molecular junctions with repeating molecular units such as benzene or phenyl rings.[13–23,70,71] These linkers provide a better opportunity to observe relationships between transport coefficients and the length of the linker. For other kinds of molecular bridges, these relationships are less distinct due to the diversity of specific properties of different parts of the bridge. Usually, these transport characteristics are measured assuming that thermal gradient $\Delta\theta$ applied across the system is much smaller than the average temperature θ characterizing the latter.[72] In this case, thermal driving forces remain relatively weak and the response of the system is linear in $\Delta\theta$. Correspondingly, transport characteristics such as electron conductance and thermopower appear to be independent on $\Delta\theta$. However, as the temperature gradient $\Delta\theta$ increases, the system may switch to a regime of operation nonlinear in $\Delta\theta$. In several recent studies, nonlinear thermoelectric transport through molecular junctions and other tailored nanoscale systems has been discussed.[35,37,43,49,58,73–76] The nonlinear Seebeck effect was already observed in semiconducting quantum dots and single molecule junctions.[19,77,78]

An important characteristic of thermoelectric transport through molecular junctions and similar nanoscale systems is the thermocurrent, defined as a difference between the charge current flowing through a biased system in the presence of a temperature gradient $\Delta\theta$ and the current flowing through the same system when the temperature gradient is removed ($\Delta\theta = 0$).[77] According to this definition, I_{th} represents the contribution to the charge current which appears due to the thermally excited transport of charge carriers through a molecular junction. The thermocurrent is more convenient for measuring and modeling than some other characteristics of thermoelectric transport such as the Seebeck coefficient. Also, it may be studied within the same computational approach over a wide range of $\Delta\theta$ values both within and beyond the linear response regime. Despite these advantages, the thermocurrent properties in nanoscale systems were not so far thoroughly studied. In accord with the well-pronounced dependences of both electron tunnel conductance and thermopower on the length of a molecular bridge, we expect I_{th} to be length-dependent as well. Also, we may expect that molecular vibrations can significantly affect thermocurrent. In the present

work, we focus on this observable and its dependences on the molecular linker length and on the effect of vibrational phonons.

II. MODEL AND MAIN EQUATIONS

In the following analysis, we assume coherent electron transmission to be the predominant transport mechanism. We simulate a linker in a single-molecule junction by a periodical chain of N sites. Each single site is assigned to an on-site energy E_i and coupled to its nearest neighbors with the coupling strengths $\beta_{i-1,i}$ and $\beta_{i,i+1}$, respectively $(2 \le i \le N-1)$. Within the simplest version of this model, all on-site energies are assumed to be equal $(E_i = E_0)$ as well as all coupling parameters $(\beta_{i-1,i} = \beta_{i,i+1} = \beta)$. Such simple chain models are often used to represent molecular bridges comprising repeating units where $\pi - \pi$ coupling dominates electron transport and the parameter β characterizes the coupling between adjacent π orbitals.[79] The schematics of this model showing relevant parameters employed in further computations is presented in Fig. 1. This simple chain model may be modified by introducing gateway states different from the rest. This could be achieved by separating out two sites at the ends of the chain, setting on these terminal sites on-site energies $E_i = E_N = \epsilon$ which differ from E_0 and suggesting that these sites are coupled to their neighbors with different strength $(\beta_{1,2} = \beta_{N-1,N} = \delta)$. It was shown that gateway states may significantly affect the length dependence of the Seebeck coefficient[19,80] and similar effects may appear in the thermocurrent. Such effects can be investigated with the simple model advanced here.

The Hamiltonian of a single-molecule junction where the chain-like bridge interacts with a single vibrational mode may be written as

$$H = H_M + H_L + H_R + H_T + H_{ph}. \tag{1}$$

For a simple chain, the term H_M that represents the molecular bridge coupled to the phonon mode has the form

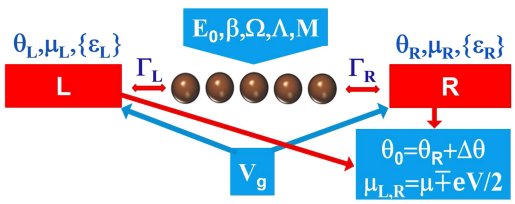

FIG. 1. Schematics of the metal-molecule-metal junction used to analyze thermally induced transport. Indicated parameters are relevant energies determining the behavior of the themocurrent.

$$H_M = E_0 \sum_{i,\sigma} d^\dagger_{i\sigma} d_{i\sigma} + \beta \sum_{i,\sigma} d^\dagger_{i\sigma} \left[d_{i+1,\sigma}(1-\delta_{iN}) + d_{i-1,\sigma}(1-\delta_{i1}) \right] + \sum_{ij\sigma} \Lambda_{ij} d^\dagger_{i\sigma} d_{j\sigma} (a^\dagger + a). \tag{2}$$

Here, $1 \le i,j \le N$, $d^\dagger_{i\sigma}$, $d_{i\sigma}$ are creation and annihilation operators for electrons with the spin σ on the bridge site "i," $a^\dagger$, a are creation and annihilation operators for the phonon mode, and δ_{ik} is the Kronecker symbol. The last term in expression (2) describes the electron-vibron interaction. In the following analysis, we assume that the coupling parameters accept nonzero values only when $i=j$ $(\Lambda_{ii} \equiv \Lambda)$ and when $i=j\pm1$ $(\Lambda_{i,i+1} = \Lambda_{i,i-1} \equiv M)$. It is reasonable to postulate that $M < \Lambda$.

The terms H_γ $(\gamma = L, R)$ correspond to noninteracting electrons on the leads with energies $\epsilon_{r\gamma\sigma}$,

$$H_\gamma = \sum_{r,\sigma} \epsilon_{r\gamma\sigma} c^\dagger_{r\gamma\sigma} c_{r\gamma\sigma}, \tag{3}$$

where $c^\dagger_{r\gamma\sigma}$ and $c_{r\gamma\sigma}$ create and annihilate electrons on the leads. Within the employed model, only terminal sites of the chain are coupled to electrodes, so the transfer Hamiltonian H_T can be written as

$$H_T = \sum_{r\sigma} (\tau_{rL\sigma} c^\dagger_{rL\sigma} d_{1\sigma} + \tau_{rR\sigma} c^\dagger_{rR\sigma} d_{N\sigma}) + H.C. \tag{4}$$

This term describes electron tunneling between the bridge and the electrodes, where factors $\tau_{r\gamma\sigma}$ characterize the coupling of relevant electron states on the bridge to those on the leads. Finally, the term H_{ph} represents the vibrational mode with the frequency Ω,

$$H_{ph} = \hbar\Omega a^\dagger a. \tag{5}$$

We note that the last term in the expression (2) may be simplified by assuming that electron-phonon coupling parameters Λ_{ii} take on the same value for all electron states on the bridge. However, this simplification is fitting well with the assumption concerning on-site energies, so we use it in following calculations. As follows from Eq. (2), interactions between electrons on the bridge are omitted from consideration. More advanced models can be used but the simple model (2) already shows the essential physics that needs to be addressed.

To eliminate the electron-phonon coupling term from the Hamiltonian (1), we employ the commonly used small polaron (Lang and Firsov) transformation which converts the Hamiltonian H_M into $\tilde{H}_M = \exp[s] H_M \exp[-s]$ where $s = \frac{\Lambda}{\hbar\Omega} \sum_{i,\sigma} d^\dagger_{i\sigma} d_{i\sigma} (a^\dagger - a) + \frac{M}{\hbar\Omega} \sum_{i,\sigma} d^\dagger_{i\sigma} [d_{i+1,\sigma}(1-\delta_{iN}) + d_{i-1,\sigma}(1-\delta_{i1})](a^\dagger - a)$.[81,82] As a result, we obtain

$$\tilde{H}_M = \tilde{E}_0 \sum_{i,\sigma} d^\dagger_{i\sigma} d_{i\sigma} + \tilde{\beta} \sum_{i,\sigma} d^\dagger_{i\sigma} \times \left[d_{i+1,\sigma}(1-\delta_{iN}) + d_{i-1,\sigma}(1-\delta_{i1}) \right]. \tag{6}$$

Here, the on-site energy acquires a polaronic shift originating from electron-vibron interaction: $\tilde{E}_0 = E_0 - \Lambda^2/\hbar\Omega$. Assuming a sufficiently weak electron-phonon coupling $(\Lambda \ll \beta)$, the coupling parameter β is renormalized in a similar way: $\tilde{\beta} = \beta - 2\Lambda M/\hbar\Omega$.

The transfer Hamiltonian (6) also undergoes a transformation. Within the accepted model, the second term in the expression for the operator "s" commutes with H_T. Thus H_T transformation reduces to the substitution of renormalized coupling parameters $\tilde{\tau}_{r\beta\sigma}$ for $\tau_{r\beta\sigma}$,

$$\tilde{\tau}_{r\beta\sigma} = \tau_{r\beta\sigma} X \equiv \tau_{r\beta\sigma} \exp\left[-\frac{\Lambda}{\hbar\Omega}(a^\dagger - a)\right]. \tag{7}$$

In addition to the Hamiltonian (1)–(5), we assume that the vibrational mode is coupled to a thermal phonon bath and that this coupling is strong enough so that the phonon maintains its thermal equilibrium state throughout the process. Consequently, the expectation value of the phonon operator X may be presented as follows:[83]

$$\langle X\rangle = \exp\left[-\left(\frac{\Lambda}{\hbar\Omega}\right)^2\left(N_{ph}+\frac{1}{2}\right)\right], \tag{8}$$

where N_{ph} denotes the equilibrium phonon population. Here, we consider the low temperature regime where $k\theta \ll \Lambda, \hbar\Omega$, so $\langle X\rangle$ may be approximated by $\exp\left[-\frac{1}{2}\left(\frac{\Lambda}{\hbar\Omega}\right)^2\right]$, which does not depend on temperature. By replacing X by $\langle X\rangle$, we decouple electron and phonon subsystems. Then the electron Green's function on the Keldysh contour may be approximated as a product of the pure electronic term computed basing on the Hamiltonian $\tilde{H} = \tilde{H}_M + \tilde{H}_T$ ($\tilde{H}_T$ being the transformed transfer Hamiltonian) and the Franck-Condon factor,[37,38,84,85]

$$G_{i\sigma,j\sigma'}(t,t') \approx -\frac{i}{\hbar}\langle T_c d_{i\sigma}(t) d^\dagger_{j\sigma'}(t')\rangle_{\tilde{H}}\langle X(t)X^\dagger(t')\rangle \equiv \tilde{G}_{i\sigma,j\sigma'}(t,t')K(t,t'). \tag{9}$$

This approximation is the most sensitive step in the accepted computational approach. It is inherent within the Born-Oppenheimer approximation and justified when a significant difference occurs between time scales characterizing electronic and vibrational dynamics. In the processes involving electron transport through molecules, this difference in time scales is by no means obvious. However, it was shown that the Born-Oppenheimer approximation in the diabatic representation may be employed in the analysis of such processes as well,[86] and this is how the approximations (9) may be understood.

The Fourier transform of the retarded Green's function for the electrons on the bridge may then be found in the form

$$\tilde{G}_r^{-1}(E) = \begin{bmatrix} E-\tilde{E}_0-\frac{i\Gamma_L}{2} & -\tilde{\beta} & 0 & 0 & \dots & 0 \\ -\tilde{\beta} & E-\tilde{E}_0 & -\tilde{\beta} & 0 & \dots & 0 \\ 0 & -\tilde{\beta} & E-\tilde{E}_0 & -\tilde{\beta} & \dots & 0 \\ \dots & \dots & \dots & \dots & \dots & \dots \\ 0 & 0 & \dots & -\tilde{\beta} & E-\tilde{E}_0 & -\tilde{\beta} \\ 0 & 0 & \dots & 0 & -\tilde{\beta} & E-\tilde{E}_0-\frac{i\Gamma_R}{2} \end{bmatrix}. \tag{10}$$

In this expression ($\gamma = L, R$),

$$\begin{aligned}\Gamma_\gamma &= 2\pi\sum_{r,\sigma}|\tilde{\tau}_{r\gamma\sigma}|^2\delta(E-\epsilon_{r\gamma\sigma}) \\ &= \exp\left[-\left(\frac{\Lambda}{\hbar\Omega}\right)^2\right]2\pi\sum_{r,\sigma}|\tau_{r\gamma\sigma}|^2\delta(E-\epsilon_{r\gamma\sigma}) \\ &\equiv \Gamma_{\gamma 0}\exp\left[-\left(\frac{\Lambda}{\hbar\Omega}\right)^2\right].\end{aligned} \tag{11}$$

Thus the coupling between the bridge and the electrodes is reduced due to the effect of molecular vibrations, being a manifestation of the Franck-Condon physics typical to this model, which is further expressed by the dynamical term $K(t, t')$ discussed below. Within the wide band approximation, one may disregard dependences of $\Gamma_{L,R}$ on E and treat these parameters as constants. In the following calculations, we focus on a symmetrically coupled single-molecule junction: $\Gamma_L = \Gamma_R = \Gamma$. We remark that at the low temperatures considered here, this symmetry is not violated by electron-phonon interactions.

When gateway states are taken into consideration, the equation for the retarded electron Green's function accepts the form

$$\tilde{G}_r^{-1}(E) = \begin{bmatrix} E-\tilde{\epsilon}-\frac{i\Gamma}{2} & -\tilde{\delta} & 0 & 0 & \dots & 0 \\ -\tilde{\delta} & E-\tilde{E}_0 & -\tilde{\beta} & 0 & \dots & 0 \\ 0 & -\tilde{\beta} & E-\tilde{E}_0 & -\tilde{\beta} & \dots & 0 \\ \dots & \dots & \dots & \dots & \dots & \dots \\ 0 & 0 & \dots & -\tilde{\beta} & E-\tilde{E}_0 & -\tilde{\delta} \\ 0 & 0 & \dots & 0 & -\tilde{\delta} & E-\tilde{\epsilon}-\frac{i\Gamma}{2} \end{bmatrix}. \tag{12}$$

This equation is derived assuming that the bridge chain is symmetrically coupled to the electrodes. Note that the on-site energy $\tilde{\epsilon}$ and the coupling parameter $\tilde{\delta}$ are shifted due to electron-phonon interactions in the same way as E_0 and β.

Next, consider the function K(t,t′). Since we assumed that the phonon subsystem maintains its thermal equilibrium, it can be evaluated to yield[85]

$$K(t,t') = \exp[-\Phi(t-t')], \tag{13}$$

where

$$\Phi(t'-t) = \frac{\Lambda^2}{(\hbar\Omega)^2}\left[N_{ph}(1-e^{i\Omega(t'-t)}) + (N_{ph}+1)(1-e^{-i\Omega(t'-t)})\right]. \tag{14}$$

Expanding $K(t,\ t')$ in the terms of Bessel functions, one obtains the following expression for the spectral function matrix elements:

$$A_{i\sigma,j\sigma'} = i\sum_{m=\infty}^{\infty} L_m\left[\tilde{G}^{<}_{i\sigma,j\sigma'}(E-m\hbar\Omega) - \tilde{G}^{>}_{i\sigma,j\sigma'}(E+m\hbar\Omega)\right]. \tag{15}$$

Here, the factors L_m have the form

$$L_m = \exp\left[\left(-\frac{\Lambda}{\hbar\Omega}\right)^2(2N_{ph}+1)\right]\exp\left[\frac{m\hbar\Omega}{2kT}\right] \times I_m\left[2\left(\frac{\lambda}{\hbar\Omega}\right)^2\sqrt{N_{ph}(N_{ph}+1)}\right] \tag{16}$$

and $I_m(Z)$ is the modified Bessel function of the mth order.

Specific manifestations of electron-vibron interactions in transport characteristics of molecular junctions are determined by three relevant energies. These are the coupling strengths of the electrodes to the molecular linker expressed by Γ_0, the electron-phonon coupling parameter Λ, and the thermal energies $k\theta_{L,R}$ ($\theta_{L,R}$ being the temperatures associated with the left and right electrodes). Here, we consider the situation when the system is weakly coupled ($\Gamma_0 \ll \Lambda,\ \hbar\Omega$) and the characteristic temperatures are low ($k\theta_{L,R} \ll \Gamma_0$). Also, we assume that electron-phonon coupling is rather weak ($\Lambda < \hbar\Omega$). Under these conditions, one may expect a pronounced vibrational structure to appear in the electron transmission function which may significantly affect characteristics of thermoelectric transport. Expanding the Bessel functions in power series and keeping first terms in these expansions, we get

$$L_m \approx \exp\left[-\frac{\Lambda}{\hbar\Omega}\right]^2\left(\frac{\Lambda}{\hbar\Omega}\right)^{2|m|}\frac{1}{|m|!}, \tag{17}$$

so, the expression (15) may be reduced to

$$A_{i\sigma,j\sigma'} = 2\sum_{m=-\infty}^{\infty} L_m\tilde{A}_{i\sigma,j\sigma'}(E-m\hbar\Omega). \tag{18}$$

The charge current flowing through the symmetrically coupled junction then takes the form[87]

$$I = \frac{e}{4\pi\hbar}\exp\left[\frac{\Lambda^2}{(\hbar\Omega)^2}\right]\int dE\,\mathrm{Tr}\{[f_L(E)\Gamma_L - f_R(E)\Gamma_R]A(E)\}. \tag{19}$$

Here, $f_{L,R}(E)$ are Fermi distribution functions for electrodes. In the considered system where only first and last sites on the molecular bridge are coupled to electrodes, each $N\times N$ transfer matrix $\Gamma_{L,R}$ has a single nonzero element $\Gamma_L^{1\sigma,1\sigma} = \Gamma_R^{N\sigma,N\sigma} = \Gamma$. Using this feature and expression (15) for spectral function, we may present the current I in Landauer form

$$I = \frac{e}{\pi\hbar}\int dE\tau(E)[f_L(E) - f_R(E)], \tag{20}$$

where electron transmission function equals

$$\tau(E) = \frac{\Gamma^2}{4}\sum_{m=-\infty}^{\infty} P(m)|\tilde{G}_{1N}(E-m\hbar\Omega)|^2 \tag{21}$$

and

$$P(m) = \frac{1}{|m|!}\left(\frac{\Lambda}{\hbar\Omega}\right)^{2|m|}. \tag{22}$$

The obtained expression for the electron transmission describes the situation when an electron on the bridge with the initial energy E may absorb and/or emit phonons thus moving to a state with the energy $E \pm m\hbar\Omega$. In weakly coupled junctions ($\Gamma_0,\ \Lambda \ll \hbar\Omega$), the broadening of these states is sufficiently small for them to serve as transport channels for traveling electrons and the electron transmission may be roughly estimated as a sum of contributions from all these channels.

When the electrodes are kept at different temperatures, the on-site energies acquire corrections proportional to the thermal energy $k\Delta\theta$ (k being the Boltzmann constant) making the Green's function matrix elements temperature-dependent.[75,77] These corrections may bring noticeable changes in the electron transmission provided that on-site energies take on values comparable with $k\Delta\theta$. However, when $E_0 \gg k\Delta\theta$ which is typical for molecular junctions at sufficiently low temperatures, the effect of temperature on the Green's function becomes negligible. In further analysis, we omit these corrections thus making the Green's function and electron transmission temperature independent.

As follows from Eqs. (10) and (12), the retarded electron Green's function is represented by the $N\times N$ matrix. Solving Eq. (10), one gets an explicit expression for the matrix element G_{1N} in the case of a simple chain[79,88,89]

$$\tilde{G}_{1N}(E) = \frac{\tilde{\beta}^{N-1}}{\Delta_N(E,\Gamma)}. \tag{23}$$

Here, the determinant $\Delta_N(E,\Gamma)$ is given by

$$\Delta_N(E,\Gamma) = \frac{1}{2^{N+1}\zeta}\left[(\lambda+\zeta)^{N-1}(\lambda+\zeta+i\Gamma)^2 - (\lambda-\zeta)^{N-1}(\lambda-\zeta+i\Gamma)^2\right], \tag{24}$$

where $\lambda = E-\tilde{E}_0,\ \zeta = \sqrt{\lambda^2-4\tilde{\beta}^2}$.

When we take into consideration the gateway states, the expression for $\tilde{G}_{1N}$ accepts the form

$$\tilde{G}_{1N}(E) = \frac{\tilde{\delta}^2 \tilde{\beta}^{N-3}}{\tilde{\Delta}_N(E,\Gamma)} \tag{25}$$

and the determinant $\tilde{\Delta}_N(E,\Gamma)$ for $N \geq 3$ equals[80]

$$\begin{aligned}\tilde{\Delta}_N(E,\Gamma) = \Delta_N(E,\Gamma) + (\alpha-\lambda)(\alpha+\lambda+i\Gamma)\Delta_{N-2}(E,0) \\ + [(\tilde{\beta}^2-\tilde{\delta}^2)(\alpha+\lambda+i\Gamma) - (\alpha-\lambda)(\tilde{\beta}^2+\tilde{\delta}^2)] \\ \times \Delta_{N-3}(E,0) - (\tilde{\beta}^4-\tilde{\delta}^4)\Delta_{N-4}(E,0).\end{aligned} \tag{26}$$

In this expression, $\alpha = \tilde{E}_0 - \tilde{\epsilon}$, $\Delta_N(E,\Gamma)$ is given by Eq. (24) and other determinants values are obtained from Eq. (24) by putting $\Gamma = 0$. In particular, $\Delta_0(E, 0) = 1$ and $\Delta_{-1}(E, 0) = 0$.

In the following analysis, we assume that the temperature of the right electrode is kept constant whereas the temperature of the left electrode varies. Also, we assume that $\theta_L > \theta_R$, so $\Delta\theta = \theta_L - \theta_R > 0$. According to its definition, the thermocurrent is given by

$$I_{th}(V) = I(V, \theta_R, \Delta\theta) - I(V, \theta_R, \Delta\theta = 0), \tag{27}$$

where V is the bias voltage applied across the junction and the Fermi functions $f_{L,R}$ are computed for different leads temperatures and for different chemical potentials $\mu_{L,R}$ of the leads. The chemical potentials are shifted with respect to each other by the bias voltage. We suppose that V is symmetrically distributed between the electrodes, so $\mu_{L,R} = \mu \mp eV/2$, μ being the chemical potential of electrodes in an unbiased system. As the electron charge is negative, a positive bias voltage shifts μ_L above μ_R. Within the accepted approximations, electron transmission $\tau(E)$ included in the integrand in Eq. (20) is temperature independent and is given by Eq. (21). We apply Eqs. (18)–(26) to analyze the dependence of the thermocurrent on the molecular bridge length.

III. RESULTS AND DISCUSSION

Consider first the case where the molecular vibrations do not affect electron transport through the system. Then the expression for the electron transmission takes the simple form

$$\tau(E) = \frac{\Gamma_0^2}{4}|\tilde{G}_{1N}(E)|^2. \tag{28}$$

In the following computations concerning the bridge with gateway states, we use $E_0 = -4.47$ eV, $\epsilon = -1.85$ eV, $\Gamma_0 = 2.85$ eV, $\delta = 1.27$ eV, and $\beta = 2.28$ eV. These are the values that were derived for single-molecule junctions with gold leads and oligophenyl bridges.[19] For a simple tight-binding chain, we put $E_0 = -4.6$ eV, $\beta = 2.2$ eV, and $\Gamma_0 = 3$ eV. We use two close sets of relevant parameters to better elucidate the effect of gateway states on the thermocurrent. In both cases, the HOMO appears to be located slightly below the chemical potential of electrodes in the unbiased system ($\mu = 0$) and, therefore, serves as the primary channel for the thermally induced transport. Consequently, the charge carriers pushed through the system from the left (hot) to the right (cool) electrode by the thermal gradient $\Delta\theta$ are holes, and the thermocurrent I_{th} through an unbiased junction takes on positive values. Obviously, the thermocurrent increases with $\Delta\theta$. This dependence is linear for small $\Delta\theta$ but it becomes superlinear at higher thermal bias, as presented in Fig. 2.

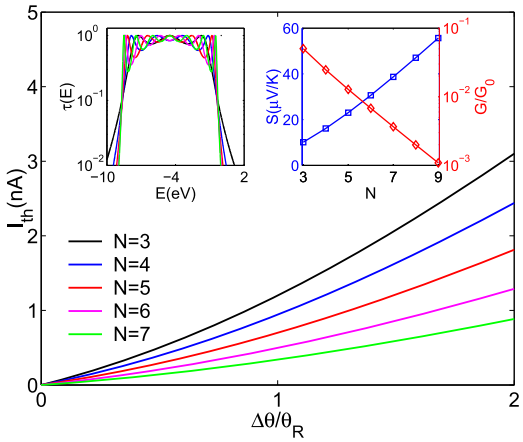

FIG. 2. Thermally excited current I_{th} in an unbiased molecular junction as a function of temperature for different lengths of the molecular bridge (different number of sites on the bridge chain). Insets show the electron transmission for a simple chain plotted as a function of tunnel energy (left) and the length dependences of the molecular conductance G and the thermopower S (right). All curves are plotted for $k\theta_R = 6$ meV, $\mu = 0$, $E_0 = -4.6$ eV, $\beta = 2.2$ eV, and $\Gamma_0 = 3$ eV.

Turning now to the bridge-length dependence of the thermocurrent, Figs. 2 and 3 show that I_{th} decreases, for a given $\Delta\theta$, when the bridge length N increases. This may be contrasted with the observation[13,15–19] that the Seebeck coefficient increases with bridge length. This apparent contradiction may be resolved by turning to the length dependence of the bridge conductance G. The latter falls very rapidly with increasing bridge length, and this fall is typically much more pronounced than the corresponding increase in the thermopower S. An example of comparative behavior of these characteristics is displayed in Fig. 2 (see the right inset). The curves plotted in the inset are computed using the expressions[90]

$$G = \frac{e^2}{\pi\hbar}\tau(\mu) \equiv G_0\tau(\mu), \tag{29}$$

$$S = \frac{\pi^2 k^2 \theta_R}{3e\tau(\mu)}\frac{\partial\tau(E)}{\partial E}\Big|_{E=\mu}. \tag{30}$$

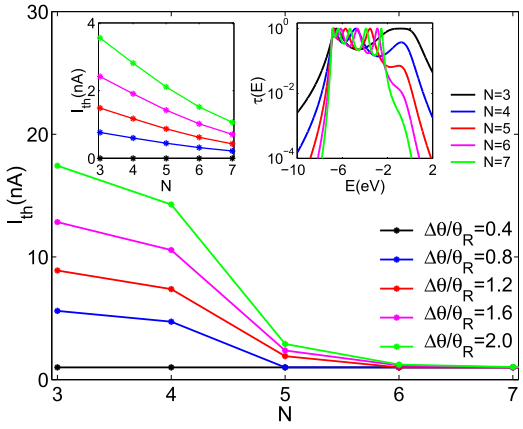

FIG. 3. The effect of gateway states on the length-dependent thermally excited current for different values of $\Delta\theta$. Curves are plotted assuming $k\theta_R = 6$ meV, $\mu = 0$, $E_0 = -4.47$ eV, $\beta = 1.27$ eV, $\Gamma_0 = 2.85$ eV, and $\delta = 2.28$ eV. Insets show I_{th} as a function of the bridge length for a simple chain computed using the same values for relevant parameters as in Fig. 2 (left) and the effect of gateway states on the electron transmission function (right).

These expressions satisfactory describe G and S at low temperatures provided that the transmission $\tau(E)$ smoothly varies in the close vicinity of the chemical potential μ: ($|E-\mu| < k\theta_R$). So, the weakening of I_{th} originates from the exponential fall of the molecular conductance, and it may appear simultaneously with the rise of the thermopower.

Electron transport driven by a thermal gradient through an unbiased single-molecule junction is dominated by a single HOMO/LUMO. The dependence of thermoelectric transport characteristics (including I_{th}) on the molecular bridge length results from the fact that the peak in $\tau(E)$ associated with the transmitting becomes sharper and narrower as the length of the molecular bridge increases. The accepted values of relevant energies result in asymmetry of the model for no energy levels appear above the Fermi level. This asymmetry was deliberately introduced to make changes in the HOMO/LUMO profile originating from variations in the bridge length more pronounced, as it happens with terminal transmission peaks within tight-binding models. However, we remark that the sharpening of the electron transmission peaks caused by the molecule lengthening is their inherent property. One may expect this effect to be manifested irrespectively of the specific model describing molecular bridge.

When gateway states are present, significant changes in the profile of the HOMO/LUMO transmission peak may occur causing variations in the length dependences of thermoelectric transport characteristics.[19,80] In the chosen model, we may analyze changes in the thermocurrent originating from the effect of gateway states. As shown in Fig. 3 (right inset), in this case the HOMO peak in the plot of $\tau(E)$ versus E appears to be significantly broader than other resonance features. The peak broadening is especially pronounced for relatively short bridges ($N \leq 5$). The distorted HOMO profile is supposed to be responsible for nonlinear temperature dependences of thermopower observed in experiments on molecular junctions.[19] In the present case, the same HOMO distortion causes a rapid fall of I_{th} occurring when the number of sites increases from $N = 3$ to $N = 5$. For longer bridges, the distortion of the HOMO profile becomes less distinct, and the fall of I_{th} slows down. On the contrary, in the case of a simple chain, I_{th} decreases nearly uniformly as the chain lengthens.

To further elucidate the nature of electron transport controlled by a thermal bias, we assume that the gate voltage V_g is applied to the junction, which shifts molecular bridge energy levels upwards along the energy scale. As follows from $\tau(E)$ profiles shown in Figs. 2 and 3, at small V_g magnitudes, the electron conduction remains low, and I_{th} takes on low values (see the inset in Fig. 4). As V_g increases, transport channels associated with higher conductance come into play bringing a significant increase in the thermocurrent magnitude. When a certain molecular level approaches the electrodes chemical potential μ from below, this level starts to serve as a transport channel for holes pushed by the thermal bias from the left (hot) electrode to the right (cool) one. Accordingly, the thermocurrent takes on positive values. When this level crosses $E = \mu$, the holes flow becomes counterbalanced by the electrons flow in the same direction, and I_{th} equals zero. When the molecular level is shifted slightly above $E = \mu$, it

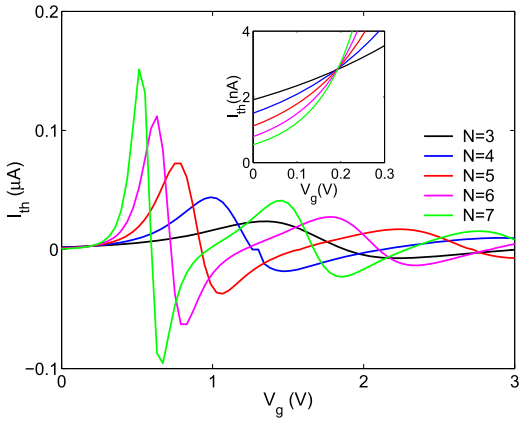

FIG. 4. Thermocurrent as a function of gate voltage V_g plotted at $k\theta_R = 6$ meV and $\Delta\theta/\theta_R = 1.4$ for several different lengths of the molecular bridge. The inset shows I_{th} vs V_g plotted at small values of V_g. All remaining relevant parameters used in plotting the curves have the same values as those used in Fig. 2.

serves as a transport channel for electrons, so I_{th} accepts negative values. As a result, a derivative-like feature appears in the I_{th} versus V_g plot. The electron transport induced by a thermal gradient applied across an electrically unbiased junction occurs solely on the condition that the molecular orbital serving as a transport channel is located in a close proximity of the electrodes chemical potential. Therefore, when the molecular energy level is shifted farther upwards, away from $E = \mu$, it ceases to serve as a transport channel.

As the gate voltage increases, another molecular energy level may approach the chemical potential bringing another derivative-like feature into the I_{th} versus V_g plot. The resulting $I_{th}(V_g)$ behavior for our model bridge is shown in Fig. 4. When the transmission peaks are well separated, the total number of derivative features is equal to the number of bridge states, namely, the number of bridge sites.

When $V_g = 0$ and a bias voltage V is applied across the system, electron transport is simultaneously driven by electric and thermal biases. The magnitude of I_{th} is determined by $\Delta\theta$ regardless of the electrical bias strength and polarity provided that the bias is sufficient for molecular orbitals associated with relatively high electron conductance to appear in the conduction window. Its sign, however, depends on the voltage bias. Each time a molecular transmission channel crosses μ, the sign of I_{th} changes, imparting an oscillatory contribution to the overall current. The thermocurrent defined by Eq. (27) represents a relatively small part of the total charge current I induced by the combined action of electrical and thermal driving forces even in weakly electrically biased molecular junctions. This is illustrated in Fig. 5.

Similar oscillations of electrical conductance and thermopower were studied for multilevel quantum dots weakly coupled to electrodes.[59,91,92] Thermopower oscillations accompanying varying chemical potential of the electrodes were observed in single-molecule junctions.[93] It was shown that Coulomb interactions between electrons on a multilevel dot significantly affect oscillations of electron transport characteristics in these systems, whereas in the present work, we did not take these interactions into account. Nevertheless, we believe that the main reason for these oscillations and

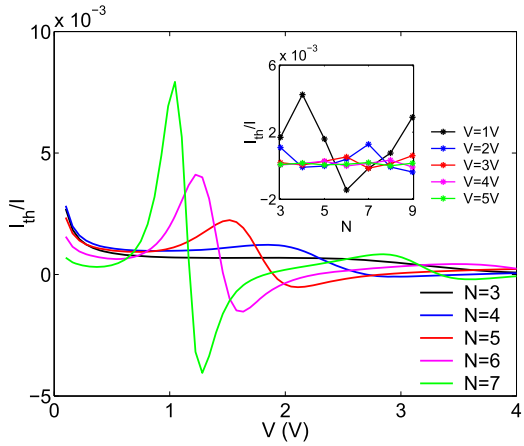

FIG. 5. The ratio of thermocurrent I_{th} computed assuming that $k\theta_R = 6$ meV and $\Delta\theta/\theta_R = 1.4$ and charge current I flowing through the junction kept at a uniform temperature ($k\theta_L = k\theta_R = 6$ meV) as a function of bias voltage. Curves are plotted for several different lengths of the molecular bridge. The inset shows I_{th}/I length dependences at several values of the bias voltage. All remaining relevant parameters used in plotting the curves have the same values as those used in Fig. 2.

quasi-oscillations of I_{th} described here is the same. These features appear when molecular orbitals (or quantum dot levels) cross the boundaries of the conduction window. The latter may be created in different ways and obviously different reasons may cause the shift of energy levels of the quantum dot and/or molecule.

As discussed before, in a weakly coupled system, the effect of vibronic interactions may be analyzed by considering the contribution of different vibronic levels to the transmission. This leads to the appearance of the vibronic structure in the transmission function (observed in inelastic tunneling spectroscopy) and to the corresponding effect on the thermal conductance. In Fig. 6, we display the transmission function $\tau(E)$ calculated using Eq. (21) for a 3-site bridge ($N = 3$). One observes that in the presence of electron-vibron interactions, each of the three electronic transmission peaks is replaced by a set of narrower peaks associated with the vibronic levels. The center of each set is shifted with respect to the original peak position. This happens due to the polaronic shift of energy levels on the bridge. These changes in the electron transmission profile take place over the whole range of relevant values of the tunnel energy E, including the interval around $E = \mu$. As before, we assume that $\mu = 0$. As shown in Fig. 6, the profile of $\tau(E)$ near $E = \mu$ may be significantly distorted. The $\tau(E)$ profile varies depending on the electron-phonon coupling strengths Λ and M as well as on the number of bridge sites and the phonon mode frequency.

These variations are expected to be most strongly pronounced in the characteristics of thermally induced electron transport through unbiased molecular junctions since in this case, the conduction window around $E = \mu$ is very narrow. One may expect alterations in molecular conduction and thermocurrent behavior to appear. For example, the length-dependent molecular conductance through a simple chain may be partly suppressed as Λ and M increase as displayed in Fig. 6. The thermocurrent itself shows changes in behavior reflecting the effect of electron-vibron coupling (see Fig. 7). One sees that I_{th} may display a minimum and/or a derivative-like feature at certain values of Λ provided that the molecular bridge includes five or more sites, that is, the bridge is sufficiently long. These features are signatures of vibronic levels appearing in the electron transmission. When the electron-phonon interaction becomes sufficiently large, these features disappear. This happens because with an increase in the coupling strengths Λ, M is accompanied by the increase of the polaronic shift (assuming that $\hbar\Omega$ remains fixed) and by the decrease in the parameter β which narrows down the energy range where $\tau(E)$ values are not too small. As a result, all transmission peaks slide to the left, leaving solely smoothly falling tails within the vicinity of $E = \mu$. Also, one may observe changes in the I_{th} dependences on the bridge length (see the inset) which appear due to the effect of the vibrational mode. We note that Eqs. (10), (21), and (22) were derived assuming a simple tight-binding model for the molecular linker. Nevertheless, these expressions give a reasonable approximation for the electron transmission which is suitable for the semiqualitative analysis of the response of thermocurrent to molecular vibrations.

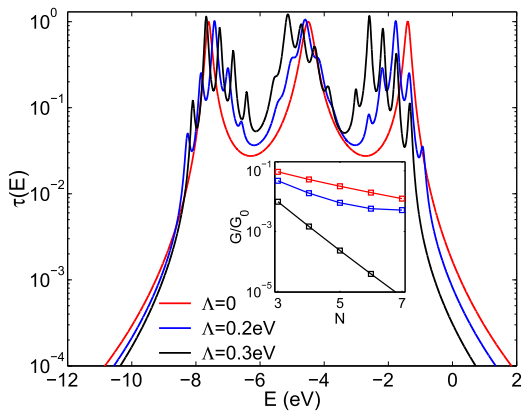

FIG. 6. Electron transmission through a junction with a chain-like bridge affected by electron-phonon interactions. Inset shows the effect of these interactions on the molecular bridge conductance. Curves are plotted for $N = 3$, $\Gamma_0 = 0.2$ eV, $\hbar\Omega = 0.42$ eV, and $M = 0.2\Lambda$. Remaining parameters take on the same values as those used in Fig. 2.

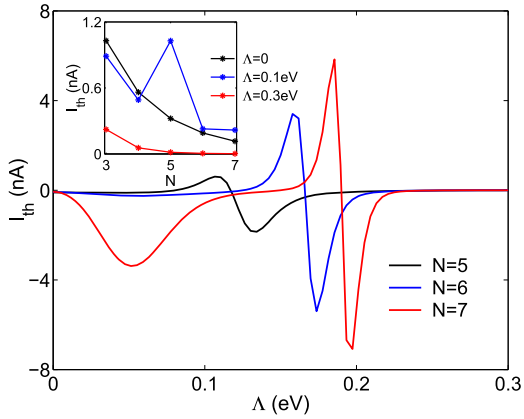

FIG. 7. Thermocurrent in the unbiased molecular junction as a function of electron-vibron coupling strength plotted for different bridge lengths. Inset shows length-dependent I_{th} at different values of Λ. All curves are plotted assuming that $k\theta_R = 6$ meV, $\Delta\theta/\theta_R = 2$, $\Gamma_0 = 0.2$ eV, $\hbar\Omega = 0.42$ eV, $E_0 = -4.6$ eV, $\beta = 2.2$ eV, $\mu = 0$, and $M = 0.2\Lambda$.

IV. CONCLUSION

In this work, we have studied some aspects of steady thermoelectric transport through a single-molecule junction with a chain-like linker of an arbitrary length. Specifically, we focus on the thermocurrent I_{th}, defined as the change in the charge current at a given bias voltage V due to an imposed temperature difference between the two leads. To compute I_{th}, we model the bridge as a tight binding chain of identical sites. We have highlighted several characteristics properties of the thermocurrent:

(a) In unbiased systems characterized by tunneling conductance, I_{th} decreases with increasing bridge length. This behavior is caused by the exponential fall of the bridge conductance with increasing bridge length.

(b) The length dependence of I_{th} may be significantly affected by the profile of the HOMO/LUMO peak in the electron transmission function. Specifically, the particular HOMO profile caused by the gateaway states associated with terminal sites on the molecular bridge may significantly change the behavior of the length-dependent thermocurrent. Similar effect of gateaway states on the thermopower of single molecule junctions was observed and analyzed in earlier studies.[19,80] We have shown that I_{th} may experience the gateaway states influence within a wide range of temperature variations.

(c) When gate or bias potentials bring the system closer to resonance transmission I_{th}, its bridge length dependence is affected by the energy dependent variations in the electron transmission profile near the electrodes Fermi energy. In a gated/biased molecular junction, the thermocurrent changes sign several times, as the voltage increases. The profile $I_{th}(V_g)$ or $I_{th}(V)$ looks like a sequence of peaks and dips. The number of peaks in this picture corresponds to the number of conducting bridge states, which in the considered model reflects the number of sites on the bridge chain. This change in the sign indicates the change of charge carriers (electron/holes) involved in the transport process. It happens when a certain molecular orbital crosses the boundary of the conduction window when either the bias or gate voltage increases. These peaks become more pronounced as the temperature gradient rises. However, at a sufficiently strongly gated/biased system when all molecular orbitals cross the boundary $E = \mu$ or are situated inside the conduction window, I_{th} becomes zero.

(d) Within our model, we have analyzed the effect of molecular vibrations on the thermocurrent. In particular, we have found that in weakly coupled molecular junctions (Λ, $\Gamma_0 \ll \hbar\Omega$) at sufficiently low temperatures (Λ, $\Gamma_0 \gg k\theta$), electron interactions with vibrational modes may qualitatively change the length dependences of I_{th}. Specifically, it was shown that I_{th} may display dips and/or derivative-like features at certain values of electron-phonon coupling parameters. These features may appear in systems with sufficiently long molecular bridges ($N \geq 5$), at sufficiently weak electron-phonon coupling ($\Lambda < \hbar\Omega$). They are signatures of vibronic levels occurring in the electron transmission.

The system used in the present analysis is simple, and more detailed models, both regarding the molecular electronic structure and its coupling to the environment, are required for quantitative calculations of thermocurrent through long molecular bridges. Nevertheless, we believe that the results presented and discussed here capture some essential physics and may be helpful in studies of thermoelectric transport through tailored nanoscale systems.

ACKNOWLEDGMENTS

We thank G. M. Zimbovsky for help with the manuscript preparation. This work was supported by the U.S. NSF-DMR-PREM 1523463 and the U.S. NSF Grant No. CHE1665291.

[1] N. Agrait, A. L. Yeyati, and J. M. Van Ruitenbeek, Phys. Rep. **377**, 81–273 (2003).
[2] J. C. Cuevas and E. Scheer, *Molecular Electronics: An Introduction to Theory and Experiment* (World Scientific, Singapore, 2010).
[3] N. A. Zimbovskaya and M. R. Pederson, Phys. Rep. **509**, 1 (2011).
[4] M. Zebarjadi, K. Esfarjani, M. S. Dresselhaus, Z. F. Ren, and G. Chen, Energy Environ. Sci. **5**, 5147 (2012).
[5] Y. Dubi and M. Di Ventra, Rev. Mod. Phys. **83**, 131 (2011).
[6] B. Sothmann, D. Sanchez, and A. N. Jordan, Nanotechnology **26**, 032001 (2015).
[7] H. Sadeghi, S. Sangtarash, and C. J. Lambert, Nano Lett. **15**, 7467 (2015).
[8] Z. Golsanamlou, M. B. Tagani, and H. R. Soleimani, Chin. Phys. B **24**, 108402 (2015).
[9] M. Noori, H. Sadeghi, and C. Lambert, Nanoscale **9**, 5299 (2017).
[10] C. A. Perroni, D. Ninno, and V. Cataudella, J. Phys.: Condens. Matter **28**, 373001 (2016).
[11] N. Yang, X. Xu, G. Zhang, and B. Li, AIP Adv. **2**, 041410 (2012).
[12] N. A. Zimbovskaya, J. Phys.: Condens. Matter **28**, 183002 (2016).
[13] F. Pauly, J. K. Viljas, and J. C. Cuevas, Phys. Rev. B **78**, 035315 (2008).
[14] C. M. Finch, V. M. Garcia-Suarez, and C. J. Lambert, Phys. Rev. B **79**, 033405 (2009).
[15] P. Reddy, S. Y. Jang, R. A. Segalman, and A. Majumdar, Science **315**, 1568 (2007).
[16] J. A. Malen, P. Doak, K. Baheti, T. D. Tilley, R. A. Segalman, and A. Majumdar, Nano Lett. **9**, 1164 (2009).
[17] S. Y. Quek, H. J. Choi, S. G. Louie, and J. B. Neaton, ACS Nano **5**, 551 (2011).
[18] A. Tan, J. Balachandran, S. Sadat, V. Gavini, B. D. Dunietz, S.-Y. Jang, and P. Reddy, J. Am. Chem. Soc. **133**, 8838 (2011).
[19] J. R. Widawsky, W. Chen, H. Vazquez, T. Kim, R. Breslow, M. S. Hybertsen, and L. Venkataraman, Nano Lett. **13**, 2889 (2013).
[20] R. X. Li, Y. Ni, H. D. Li, X. L. Tian, K. L. Yao, and H. H. Fu, Phys. B **493**, 1 (2016).
[21] Z. Golsanamlou, S. I. Vishkayi, M. B. Tagani, and H. R. Soleimani, Chem. Phys. Lett. **594**, 51 (2014).
[22] O. Karlstrom, M. Strange, and G. C. Solomon, J. Chem. Phys. **140**, 044315 (2014).
[23] M. Tsutsui, K. Yokota, T. Morikawa, and M. Taniguchi, Sci. Rep. **7**, 44276 (2017).
[24] R. N. Wang, X. H. Zheng, Z. X. Dai, H. Hao, L. L. Song, and Z. Zeng, Phys. Lett. A **375**, 657 (2011).
[25] P. Murphy, S. Mukerjee, and J. Moore, Phys. Rev. B **78**, 161406(R) (2008).
[26] B. Kubala, J. Konig, and J. Pekola, Phys. Rev. Lett. **100**, 066801 (2008).
[27] D. Nozaki, H. Sevincli, W. Li, R. Gutierrez, and G. Cuniberti, Phys. Rev. B **81**, 235406 (2010).
[28] A. L. Monteros, G. S. Uppal, S. R. McMillan, M. Crisan, and I. Tifrea, Eur. Phys. J. B **87**, 302 (2014).
[29] N. A. Zimbovskaya, J. Chem. Phys. **140**, 104706 (2014).
[30] J. Azema, A.-M. Dare, S. Schafer, and P. Lombardo, Phys. Rev. B **86**, 075303 (2012).
[31] Y. Yan, H. Wu, F. Jiang, and H. Zhao, Eur. Phys. J. B **87**, 244 (2014).
[32] M. A. Sierra, M. Saiz-Bretin, F. Dominguez-Adame, and D. Sanchez, Phys. Rev. B **93**, 235452 (2016).

[33]Y. W. Chang and B. Y. Jin, J. Chem. Phys. **141**, 064111 (2014).
[34]Y. W. Chang and B. Y. Jin, J. Chem. Phys. **146**, 134113 (2017).
[35]M. Leijnse, M. R. Wegewijs, and K. Flensberg, Phys. Rev. B **82**, 045412 (2010).
[36]L. Simine and D. Segal, Phys. Chem. Chem. Phys. **14**, 13820 (2012).
[37]M. Galperin, M. A. Ratner, and A. Nitzan, Mol. Phys. **106**, 397 (2008).
[38]R. Hartle and M. Thoss, Phys. Rev. B **83**, 115414 (2011).
[39]M. Tsutsui and M. Taniguchi, J. Appl. Phys. **113**, 084301 (2013).
[40]A. Erpenbeck, R. Hartle, and M. Thoss, Phys. Rev. B **91**, 195418 (2015).
[41]N. A. Zimbovskaya, J. Phys.: Condens. Matter **28**, 295301 (2016).
[42]J. H. Ojeda, C. A. Duque, and D. Laroze, Phys. B **502**, 73 (2016).
[43]J. K. Sowa, J. A. Mol, G. A. D. Briggs, and E. M. Gauger, Phys. Rev. B **95**, 085423 (2017).
[44]J. Ren, J.-X. Zhu, J. E. Gubernatis, C. Wang, and B. Li, Phys. Rev. B **85**, 155443 (2012).
[45]K. Walczak, Phys. B **392**, 173 (2007).
[46]C. A. Perroni, D. Ninno, and V. Cataudella, Phys. Rev. B **90**, 125421 (2014).
[47]R. Hartle, M. Butzin, and M. Thoss, Phys. Rev. B **87**, 085422 (2013).
[48]J. Arguello-Luengo, D. Sanchez, and R. Lopez, Phys. Rev. B **91**, 165431 (2015).
[49]G. T. Craven and A. Nitzan, J. Chem. Phys. **146**, 092305 (2017).
[50]L. A. Zotti, M. Burkle, F. Pauly, W. Lee, K. Kim, W. Jeong, Y. Asai, P. Reddy, and J. C. Cuevas, New J. Phys. **16**, 015004 (2014).
[51]T. Koch, J. Loos, and H. Fehske, Phys. Rev. B **89**, 155133 (2014).
[52]B. De and B. Muralidharan, Phys. Rev. B **94**, 165416 (2016).
[53]N. A. Zimbovskaya, Phys. E **74**, 213 (2015).
[54]N. A. Zimbovskaya, J. Phys.: Condens. Matter **26**, 275303 (2014).
[55]P. Trocha and J. Barnas, Phys. Rev. B **85**, 085408 (2012).
[56]L. Simine, W. J. Chen, and D. Segal, J. Phys. Chem. C **119**, 12097 (2015).
[57]N. R. Abdullah, C. S. Tang, A. Manolescu, and V. Gudmundsson, ACS Photonics **3**, 249 (2016).
[58]M. Wierzbicki and R. Swirkowicz, Phys. Rev. B **82**, 165334 (2010).
[59]R. Swirkowicz, M. Wierzbicki, and J. Barnas, Phys. Rev. B **80**, 195409 (2009).
[60]L. Karwacki and P. Trocha, Phys. Rev. B **94**, 085418 (2016).
[61]L. Xu, Z. J. Li, P. Niu, and Y. H. Nie, Phys. Lett. A **380**(42), 3553 (2016).
[62]J. Fransson and M. Galperin, Phys. Rev. B **81**, 075311 (2010).
[63]J. Fransson and M. Galperin, Phys. Chem. Chem. Phys. **13**, 14350 (2011).
[64]S. Weiss, J. Bruggemann, and M. Thorwart, Phys. Rev. B **92**, 045431 (2015).
[65]D. Aravena and E. Ruiz, J. Am. Chem. Soc. **134**, 777 (2012).
[66]K. Uchida, M. Ishida, T. Kikkawa, A. Kirihara, T. Murakami, and E. Saitoh, J. Phys.: Condens. Matter **26**, 343202 (2014).
[67]K. Xu, J. Huang, Z. Guan, Q. Li, and J. Yang, Chem. Phys. Lett. **535**, 111 (2012).
[68]E. Cremades, C. D. Pemmaraju, S. Sanvito, and E. Ruiz, Nanoscale **5**, 4751 (2013).
[69]B. Szukiewicz and K. I. Wysokinski, Eur. Phys. J. B **88**, 112 (2015).
[70]M. Wang, X. Shan, and N. Yang, Phys. Lett. A **376**, 3514 (2012).
[71]Y.-H. Wang, X.-Y. Zhou, Y.-Y. Sun, D. Han, J.-F. Zheng, Z.-J. Niu, and X.-S. Zhou, Electrochim. Acta **123**, 205 (2014).
[72]L. Rincon-García, C. Evangeli, G. Rubio-Bollinger, and N. Agrait, Chem. Soc. Rev. **45**, 4285 (2016).
[73]Y. Dubi and M. Di Ventra, Nano Lett. **9**, 97 (2009).
[74]J. Azema, P. Lombardo, and A.-M. Dare, Phys. Rev. B **90**, 205437 (2014).
[75]R. Lopez and D. Sanchez, Phys. Rev. B **88**, 045129 (2013).
[76]D. Sanchez and R. Lopez, C. R. Phys. **17**, 1060 (2016).
[77]S. F. Svensson, E. A. Hoffmann, N. Nakpathomkun, P. M. Wu, H. Q. Xu, H. A. Nilsson, D. Sanchez, V. Kashcheyevs, and H. Linke, New J. Phys. **15**, 105011 (2013).
[78]Y. Kim, A. Lenert, E. Meyhofer, and P. Reddy, Appl. Phys. Lett. **109**, 033102 (2016).
[79]D. Nozaki, H. M. Pastawski, and G. Cuniberti, New J. Phys. **12**, 063004 (2010).
[80]N. A. Zimbovskaya, J. Chem. Phys. **145**, 221101 (2016).
[81]I. G. Lang and Y. A. Firsov, Zh. Eksp. Teor. Fiz. **41**, 1843 (1962) [Sov. Phys.-JETP **16**, 1301 (1963)].
[82]G. D. Mahan, *Many-Particle Physics* (Plenum, New York, 2000).
[83]O. Entin-Wohlman, Y. Imry, and A. Aharony, Phys. Rev. B **81**, 113408 (2010).
[84]M. Galperin, A. Nitzan, and M. A. Ratner, Phys. Rev. B **73**, 045314 (2006).
[85]R. Swirkowicz, M. Wilczynski, and J. Barnas, J. Phys.: Condens. Matter **20**, 255219 (2008).
[86]A. Nitzan, *Chemical Dynamics in Condensed Phases* (Oxford University Press, Oxford, 2006).
[87]M. Cizek, M. Thoss, and W. Domcke, Phys. Rev. B **70**, 125406 (2004).
[88]V. Mujica, M. Kemp, and M. A. Ratner, J. Chem. Phys. **101**, 6849 (1994).
[89]J. L. D'Amato and H. M. Pastawski, Phys. Rev. B **41**, 7411 (1990).
[90]M. Paulsson and S. Datta, Phys. Rev. B **67**, 241403(R) (2003).
[91]C. W. J. Beenakker and A. A. M. Staring, Phys. Rev. B **46**, 9667 (1992).
[92]Y.-C. Chang and D. M.-T. Kuo, Phys. Rev. B **77**, 245412 (2008).
[93]T. Morikawa, A. Arima, M. Tsutsui, and M. Taniguchi, Nanoscale **6**, 8235 (2014).